






APPLICATION ARTICLE

3D pollination biology using micro-computed tomography and geometric morphometrics in *Theobroma cacao*

Katherine A. Wolcott¹  | Edward L. Stanley²  | Osman A. Gutierrez³  |
Stefan Wuchty^{1,4,5,6}  | Barbara Ann Whitlock¹ 

¹Department of Biology, University of Miami, Coral Gables, Florida 33124, USA

²Department of Natural History, Florida Museum of Natural History, Gainesville, Florida, USA

³Subtropical Horticultural Research Station, United States Department of Agriculture–Agricultural Research Service (USDA-ARS), Miami, Florida 33158, USA

⁴Department of Computer Science, University of Miami, Coral Gables, Florida 33146, USA

⁵Institute of Data Science and Computing, University of Miami, Coral Gables, Florida 33146, USA

⁶Sylvester Comprehensive Cancer Center, University of Miami, Miami, Florida 33136, USA

Correspondence

Katherine A. Wolcott, Department of Biology, University of Miami, Coral Gables, Florida 33124, USA.

Email: kwolcott@miami.edu

This article is part of the special issue “Advances in Plant Imaging across Scales.”

Abstract

Premise: Imaging technologies that capture three-dimensional (3D) variation in floral morphology at micro- and nano-resolutions are increasingly accessible. In herkogamous flowers, such as those of *Theobroma cacao*, structural barriers between anthers and stigmas represent bottlenecks that restrict pollinator size and access to reproductive organs. To study the unresolved pollination biology of cacao, we present a novel application of micro-computed tomography (micro-CT) using floral dimensions to quantify pollinator functional size limits.

Methods: We generated micro-CT data sets from field-collected flowers and museum specimens of potential pollinators. To compare floral variation, we used 3D Slicer to place landmarks on the surface models and performed a geometric morphometric (GMM) analysis using geomorph R. We identified the petal side door (an opening between the petal hoods and filament) as the main bottleneck for pollinator access. We compared its mean dimensions with proposed pollinators to identify viable candidates.

Results: We identified three levels of likelihood for putative pollinators based on the number of morphological (body) dimensions that fit through the petal side door. We also found floral reward microstructures whose presence and location were previously unclear.

Discussion: Using micro-CT and GMM to study the 3D pollination biology of cacao provides new evidence for predicting unknown pollinators. Incorporating geometry and floral rewards will strengthen plant–pollinator trait matching models for cacao and other species.

KEYWORDS

3D Slicer, cacao, chocolate, geometric morphometrics, Malvaceae, micro-CT, pollination biology, *Theobroma*

RESUMEN

Premisa: Las tecnologías de imagen que capturan la variación tridimensional (3D) en la morfología floral en resoluciones a nivel micro y nano son cada vez más accesibles. En las flores hercógamas, tal como las de cacao (*Theobroma cacao* L.), las barreras estructurales entre las anteras y los estigmas representan cuellos de botella que restringen el tamaño de los polinizadores y el acceso a los órganos reproductivos. Para estudiar la biología de polinización del cacao que hasta estos momentos no ha sido completamente explicada, presentamos una nueva aplicación de microtomografía computarizada (microTC) que utiliza dimensiones florales para cuantificar los límites de tamaño funcional de los polinizadores.

This is an open access article under the terms of the Creative Commons Attribution-NonCommercial License, which permits use, distribution and reproduction in any medium, provided the original work is properly cited and is not used for commercial purposes.

© 2023 The Authors. *Applications in Plant Sciences* published by Wiley Periodicals LLC on behalf of Botanical Society of America.

Métodos: Generamos conjuntos de datos microTC de flores recolectadas en el campo, así como especímenes de museo de potenciales polinizadores. Para comparar la variación floral, usamos el programa 3D Slicer para colocar puntos de referencia en los modelos de superficie y realizamos un análisis morfométrico geométrico (MGM) usando el programa geomorph R. Identificamos la parte lateral de los pétalos (abertura entre las capuchas de los pétalos y el filamento) como el cuello de botella principal para el acceso de los polinizadores. Comparamos las medias de sus dimensiones con las de los polinizadores propuestos para identificar candidatos viables.

Resultados: Identificamos tres niveles de probabilidad para los supuestos polinizadores basado en el número de dimensiones morfológicas (de cuerpo) que caben a través la parte lateral de los pétalos. Encontramos microestructuras de recompensa floral a lo largo de las rutas de los polinizadores cuya presencia y ubicación no estaban muy claras anteriormente.

Discusión: El uso de microTC y GMM para estudiar la biología de polinización tridimensional (3D) del cacao proporciona nueva evidencia para predecir el tamaño de polinizadores desconocidos. La incorporación del análisis geométrico y de las microestructuras de recompensa floral fortalecerá los modelos de combinación de características de plantas y polinizadores para el cacao y otras especies.

RESUMO

Premissa: Tecnologias que usam imagem para capturar a variação tridimensional (3D) na morfologia floral em resoluções micro e nano estão cada vez mais acessíveis. Em flores hercogâmicas, tal como as do cacao (*Theobroma cacao*), barreiras estruturais entre as anteras e estigmas representam gargalos que restringem o tamanho do polinizador e o acesso aos órgãos reprodutivos. Para estudar a polinização do cacau, apresentamos uma nova aplicação de microtomografia computadorizada (microTC) usando dimensões florais para quantificar os limites de tamanho funcional de polinizadores.

Métodos: Nós geramos conjuntos de dados de microTC para flores coletadas em campo e para espécimes de museus de potenciais espécies polinizadoras. Para comparar a variação floral, usamos o software 3D Slicer para determinar pontos de referência na superfície dos modelos. Realizamos também análises de morfometria geométrica (MGM) usando o pacote geomorph no software R. Nós identificamos a abertura lateral da pétala (entre a pétala cuculada e os filamentos) como o principal gargalo para o acesso do polinizador. Por fim, comparamos as dimensões médias das flores com a dos polinizadores propostos para identificar candidatos viáveis.

Resultados: Identificamos três níveis de probabilidade para os supostos polinizadores baseados no número de dimensões morfológicas (corporais) que se ajustam à parte lateral das pétalas. Também encontramos microestructuras presentes nas flores que servem como recompensas aos polinizadores, cuja presença e localização não eram claras anteriormente.

Discussão: O uso de microTC e MGM para estudar a biologia da polinização do cacau em 3D fornece novas evidências para prevermos polinizadores desconhecidos. A incorporação de análises geométricas e microestructuras de recompensa floral poderá fortalecer modelos que combinam características da associação planta – polinizador tanto para o cacau, quanto para outras espécies.

Modern imaging technologies that can capture three-dimensional (3D) variation in floral morphology at micro- and nano-resolutions are becoming increasingly accessible. *Theobroma cacao* L. (cacao; Malvaceae), the source of chocolate and cocoa, has a complex 3D floral morphology that can be challenging to interpret. The small size of the flowers (<1 cm across) and elaborate morphology of the petals and androecium limit pollinator access and

movement within the flowers (see pollinator behavior descriptions by Posnette, 1950; Smith et al., 1985). Small insects are believed to be cacao pollinators, but there is uncertainty about the species involved (reviewed by Toledo-Hernández et al., 2017). Discerning a floral visitor from a true pollinator is not trivial, especially when the flowers and insects are only a few millimeters in size. Additionally, cacao is widely grown throughout the tropics, and many surveys

of insect floral visitors have been conducted on cultivated trees outside its native range (see, for example, Posnette, 1950; Frimpong-Anin et al., 2014; Toledo-Hernández et al., 2021). It is unlikely that the same insects are responsible for pollination of wild trees within its native range in the Americas and cultivated trees in geographically distant locations in Africa and Southeast Asia. As a result, large knowledge gaps remain in the details of cacao's pollination biology.

Cacao and chocolate derivatives are one of the world's most economically important agricultural products (\$67 billion USD in 2021; FAO, 2023), and their yields are pollinator-limited (Groeneveld et al., 2010; Toledo-Hernández et al., 2017; Chumacero de Schawe et al., 2018; Forbes et al., 2019). Amidst massive global losses of insect pollinators, novel targeted strategies to increase and improve successful cacao pollination are more important than ever (Goulson, 2019). Here, we present an innovative 3D morphological approach that uses micro-computed tomography (micro-CT) and geometric morphometrics (GMM) to investigate the possible pollinators of cacao.

Cacao trees are native to the tropical Americas, with a center of origin and domestication hypothesized to be in the upper Amazon (Zarrillo et al., 2018). Cacao is now grown throughout the wet tropics at low elevations. Its floral morphology and development have been extensively described (e.g., Cuatrecasas, 1964; Young et al., 1987; Bayer and Hoppe, 1990; Kubitzki and Bayer, 2003; Swanson, 2005; Young, 2007; Swanson et al., 2008). Cacao inflorescences are cauliflorous and borne on the trunk and branches of the trees (Figure 1A). The flowers are pentamerous (five units of symmetry), actinomorphic, and perfect, with a strong degree of herkogamy (physical separation between anthers

and stigma), while the sepals are valvate, pale, and reflexed at anthesis (Figure 1B). The five free petals have an unusual 3D form, with a rigid cucullate or hooded base. The petals are semi-translucent, pale yellow or cream colored, with two to three longitudinal nerves on the inner surface that are dark burgundy, possibly functioning as pollinator guides, and a pale ovoid to deltoid ligule extending outwards (Posnette, 1950). We recognize five pairs of fertile stamens opposite the petals, with a single filament extending from the top of the staminal tube to the petal hood, which conceals two dithecate anthers within. Some authors (e.g., Cuatrecasas, 1964) interpret the androecium as consisting of five stamens, each with two anthers. Fertile stamens and staminodes are fused at the base into a staminal tube. Five dark burgundy staminodes are located opposite the sepals and possibly function as pollinator guides. The gynoecium consists of five fused carpels. The ovaries are superior, oblong-ovoid, and pentagonal with five locules. The five styles are fused for most of their length, and glabrous. Large baccate fruits vary in shape depending on the genotype, with a thick outer shell, and contain 20–40 seeds surrounded by a sweet pulp (Cuatrecasas, 1964).

In cacao, the anthers and stigmas are physically separated. This herkogamous positioning of floral organs is hypothesized to limit and direct insect movement to promote pollination, particularly for flowers with other mechanisms in place to prevent selfing (such as the self-incompatibility observed in some populations of cacao; Webb and Lloyd, 1986). The dimensions of these pollinator paths and structural barriers that separate anthers and stigmas represent bottlenecks limiting the size of viable insect pollinators (Westerkamp et al., 2006); for example, cacao petal hoods surround the anthers so effectively that

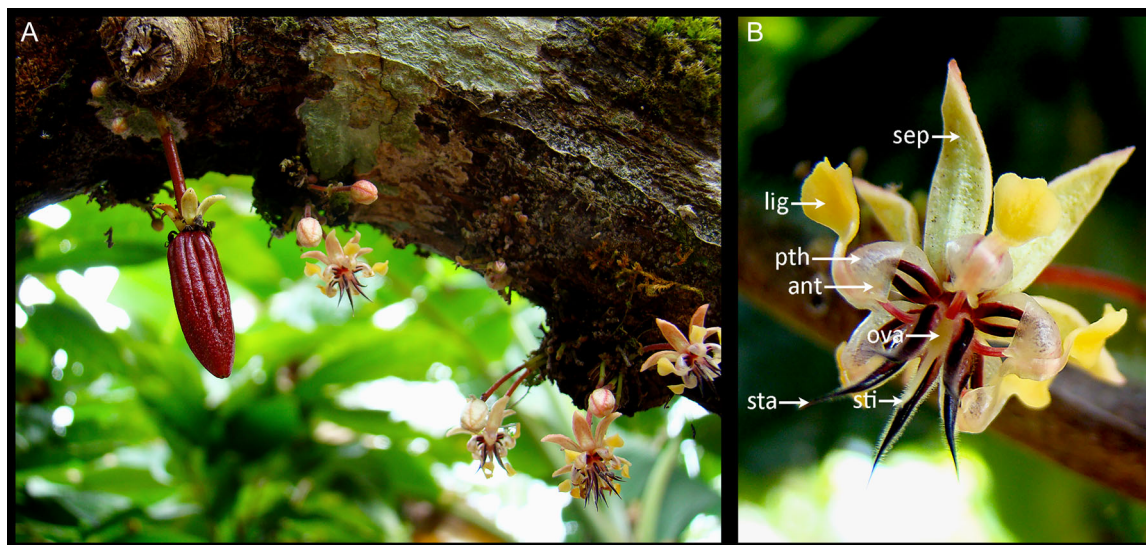


FIGURE 1 Inflorescence, flower, and pod morphology of cacao (*Theobroma cacao*). (A) Cauliflorous inflorescences and a cherelle (young pod). (B) A labeled flower. Note the translucent petal hoods (pth) with yellow ligules (lig) extending from their apex and dark red longitudinal nerves on their inner surfaces. Dark red staminodes (sta) surround the style and stigma (sti), alternating with fertile stamens. Pink filaments are visible, but the anthers (ant) are fully concealed within the petal hood. Flower dimensions are typically 10–15 mm in height. ova = ovary; sep = sepal. Photo taken at the CATIE cacao germplasm collection in Costa Rica, courtesy of USDA-ARS (Miami, Florida, USA).

the anthers are only visible when viewed from the base of the petal, not from the side or from above (in Figure 1B, note that anthers are fully concealed). There is also a temporal component to the extent of the physical separation of the anthers and stigmas. Most floral organs of cacao change position throughout anthesis, affecting pollinator movement within the flower. Stamines form a cage around the stigma that opens, closes, and re-opens throughout the day, possibly corresponding to periods of stigmatic receptivity (see splayed stamens in Figure 1B; Young et al., 1987; Swanson et al., 2008; Frimpong-Anin et al., 2014). Petal ligules transition from being vertical to horizontal (Young et al., 1984, 1987), but the petal hood position and dimensions have not been reported to change during the pollination phase of anthesis.

The floral traits of cacao are generally accepted to be consistent with myiophily (fly pollination), including the small flower size; a red, yellow, and white color palette; and a faint putrid odor (Erickson et al., 1987; Arnold et al., 2019). The pollination of cacao has been studied in cultivated trees both within and outside its native range (Salazar-Díaz and Torres-Coto, 2017; Chumacero de Schawe et al., 2018; Vansynghel et al., 2022), with small flies in the Ceratopogonidae (ceratopogonid midges, especially *Forcipomyia* spp.) and Cecidomyiidae (cecidomyiid midges) often considered the most likely pollinators based on their reported high visitation rates and ability to carry a sufficient pollen load (Young, 1985). However, some studies have observed relatively low numbers of visiting midges, and low pollen loads on those observed (see, for example, Kaufmann, 1974; Chumacero de Schawe et al., 2018; reviewed by Toledo-Hernández et al., 2017). Young (1983) reported no increase in fruit set despite increased midge population sizes, suggesting that these commonly investigated insects may be unreliable pollinators of cacao (e.g., Chumacero de Schawe et al., 2018; reviewed by Toledo-Hernández et al., 2017). It has also been proposed that any taxa of an appropriate size of about 3 mm can effectively pollinate cacao, including small dipterans and hymenopterans (Winder, 1978; Young, 1985; Young et al., 1987; Frimpong-Anin et al., 2014; Chumacero de Schawe et al., 2018; reviewed by Toledo-Hernández et al., 2017).

Floral reward structures have also been investigated for their role in cacao's pollination biology using light microscopy and scanning electron microscopy (SEM), but their presence and location are unresolved. Young et al. (1984) and Young (1985) described the presence of cacao floral reward structures in the form of glandular hairs and stomatal nectaries along the ovary and stamens, inside petal hoods, and between petal hoods and sepals. By contrast, Vogel (2000) reported an absence of floral reward structures. It has even been suggested that midges may pierce and drink from the stamens (Simpson and Neff, 1981). In lieu of rewards, it is also possible that cacao plants use a floral deceit strategy, in which olfactory and visual cues attract pollinators.

Despite the lack of clarity in which pollinator taxa are responsible and what rewards, if any, they are receiving, it is clear that pollinator behavior within and between flowers plays a role in the successful pollination of cacao. Anthers are concealed within petal hoods, and to be a successful pollinator, an insect must be able to reach the anther. We argue that combining the morphometrics of flowers and their insect visitors is an essential tool to investigate the functional limits of potential pollinators. Such novel approaches will hopefully resolve the contradictions that remain following decades of research on the pollination biology of cacao. Previous methods relied on a combination of two-dimensional imaging with landmarks and traditional morphometrics measurements using calipers (e.g., Jürgens, 2006; Rakosy et al., 2017; Wilson et al., 2017; Bilbao et al., 2021). The increasing use of 3D imaging, such as micro-CT, allows for the high-resolution study of floral organs and their internal anatomy (e.g., van der Niet et al., 2010; Dellinger et al., 2014; Wang et al., 2015; Staedler et al., 2018). When micro-CT and 3D GMM are combined to study plant-pollinator geometries, they capture the full scale of floral variation without needing to dissect or distort positional relationships (Dellinger, 2020). These methods are also more reproducible, as 3D data sets and their landmarks can be independently verified by researchers anywhere in the world. Furthermore, these methods provide a unique opportunity to compare the intricate morphologies of plants and their pollinators for the novel analysis of shapes and their evolutionary relationships (e.g., Dellinger et al., 2019; Reich et al., 2020).

Here, we use a functional approach that uses floral dimensions to quantify the functional size limits of pollinators in cacao to address its still unresolved pollination biology. We compare these floral dimensions with both commonly assumed pollinators (small ceratopogonid and cecidomyiid midges) and understudied candidate insect taxa to gain a more complete picture of pollination in cacao. Our findings could potentially be used to increase the yields and agricultural value of this globally important crop. Our efforts focus on morphologically characterizing the region surrounding the petal hood that we hypothesize acts as a bottleneck for pollen access, which we refer to as the petal side door. This entrance is also the only organ of the cacao flower whose position remains constant for the duration of anthesis, making it an ideal region to measure across flowers picked at different times of day.

METHODS

Specimen collection and sourcing

Flowers ($N=53$) were obtained from living collections of six trees at the United States Department of Agriculture-Agricultural Research Service (USDA-ARS) Subtropical Horticultural Research Station (SHRS) and Fairchild Tropical Botanic Garden (FTG) in Miami-Dade County, Florida, USA,

between January and June 2022 (Appendix S1). The flowers were removed from the tree trunks and branches at different heights, then placed in tap water before being transported to the lab, where they were fixed in formaldehyde:alcohol:acetic acid (FAA; 10%:50%:5% + 35% water) for seven days, then transferred to 70% ethanol for long-term storage following protocols reviewed by Keklikoglou et al. (2019). It is not known which genetic groups of cacao (Motamayor et al., 2008; Zhang et al., 2009; Fouet et al., 2022) our sampled trees belong to.

A selection of hypothesized pollinator taxa ($N = 10$) from the literature were sourced based on their availability from alcohol collections at the Florida Department of Agriculture and Consumer Services Division of Plant Industry (FDACS-DPI) and Florida Keys Mosquito Control (Keys Mosquito), Florida, USA (Appendix S1).

Micro-CT scanning

The fixed flowers were stained to enhance their soft tissue contrast using 1% phosphotungstic acid (PTA; w/v in 70% ethanol) for a minimum of one week and up to four months (Appendix S2; method described by Metscher, 2009; reviewed by Keklikoglou et al., 2019). Micro-computed X-ray tomography scanning (micro-CT) was performed using two different machines due to funding and time availability across the institutes involved. At the Nanoscale Research Facility (University of Florida, Gainesville, Florida, USA), a Zeiss Xradia 620 Versa (Carl Zeiss, Oberkochen, Germany) was used to scan some of the flower specimens and all insects. At the Advanced Infrastructure Materials Research Laboratory (College of Engineering, University of Miami, Coral Gables, Florida, USA), a Skyscan 1273 (Bruker, Billerica, Massachusetts, USA) was used to scan additional flowers. The scanning parameters are found in Appendix S2, with photos to accompany the specimen positioning descriptions provided in Appendix S3. Projection images were reconstructed to non-proprietary 16-bit TIFF stacks using either XMReconstructor (Carl Zeiss) or SkyScan NRecon (Bruker).

Floral GMM analysis

The reconstructed TIFF stacks of the floral and insect data sets were imported into the open-source platform 3D Slicer (Kikinis et al., 2014) using the SlicerMorph module (Rolfe et al., 2021) on a Dell XPS 8940 Desktop (64 GB RAM, NVIDIA GeForce RTX 3060, i9-11900K processor; Dell, Round Rock, Texas, USA). The data sets were segmented primarily using thresholding and masking, with the paintbrush, eraser, and remove-islands tools used to refine the separation between the flowers, scanning containers, and materials in cases of similar contrast. Flower 3D models were generated and saved as .ply files. After inspecting 10 specimens from all trees, select literature on cacao floral morphometrics (Engels, 1983; Alves et al., 2003; Bekele et al., 2006; Santos et al., 2012; Jaramillo et al., 2022),

landmark positions, and techniques of fixed versus sliding semilandmarks were determined to best capture the spatial dimensions of structures related to pollination and cacao taxonomy (Gonzalez et al., 2016; Savriama and Tautz, 2022). During our inspection, we found that many flowers had some missing or damaged parts (petals, anthers, ligules, staminodes, and/or sepals). To maximize the number of data sets eligible for landmarking and minimize introduced errors by estimating the dimensions of missing structures, one complete unit of symmetry was randomly selected for analysis per flower (one adjacent petal, sepal, ovary, and staminode). Flowers without one complete unit of floral symmetry ($n = 13$) were excluded, for a total of $N = 40$ flowers analyzed.

Fixed and sliding semilandmarks were manually applied using the Markups Module in 3D Slicer. Figure 2 shows example landmarks used for GMM ($N = 135$ per flower) in blue (light blue and dark teal). Landmarks used only to measure the cacao floral dimensions commonly reported in the literature ($N = 25$ per flower) are shown in yellow. Light blue semilandmarks ($N = 80$) measure the staminode tube length, adaxial filament length, ligule length, ligule width, sepal length, and sepal width. Dark teal semilandmarks ($N = 55$) measure the left/right petal perimeters (LP/RP) and abaxial filament length (AF). These structures represent our hypothesized spatial bottleneck to cacao pollination, which we call the petal side door (shown in Figure 2B). The petal side door dimensions (PSD) used for a downstream pollinator size analysis were calculated by summing the average petal perimeter length with the abaxial filament length ($PSD_{dim} = (LP_{perim} + RP_{perim})/2 + AF_{len}$). Fixed landmark points shown in yellow ($N = 5$) measure the ovary bottom, ovary top, stigma bottom, stigma top, and position on the staminode closest to the stigma top, and semilandmarks ($N = 20$) measure the ovary perimeter (Figure 2C).

The GMM analysis was used to quantify the variation among flowers prior to determining the mean spatial dimensions of the petal side door, used for downstream comparisons with insect dimensions. The landmarks were exported to .mrk.json to preserve the metadata and subsequently imported into R version 4.0.5 (R Core Team, 2021) with SlicerMorphR version 0.0.0.9000 (Rolfe et al., 2021) for analysis using geomorph version 4.0.5 (Adams and Otárola-Castillo, 2013). A generalized Procrustes analysis (GPA) was used to align and scale the landmark data sets with geomorph gpgen. The mean reference shape was calculated using mshape. A principal component analysis (PCA) was performed on aligned and scaled data sets to quantify the shape variation among flowers when compared with the mean reference shape using geomorph gm.prcomp. Figures were created using geomorph plotting functions (plotRefToTarget, plotOutliers) and ggplot2 (Wickham, 2016). A one-way Procrustes analysis of variance (ANOVA) was used to test for the effects of tree self-compatibility, tree individual, collection month, and flower size (centroid size) on floral shape. The code used for the analysis and figure generation, along with the landmark files, are available on GitHub (https://github.com/aubricot/Cacao_3D_gmm; see Data Availability Statement).

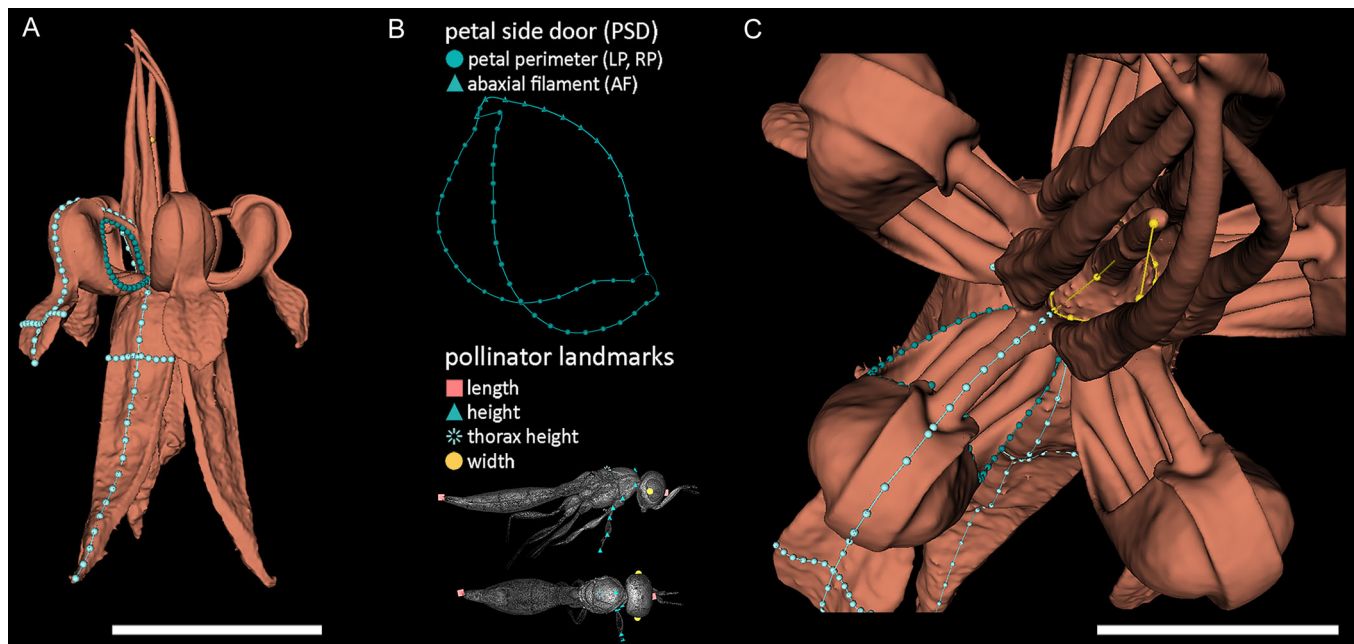


FIGURE 2 Floral fixed and sliding semilandmarks used to study the 3D pollination biology of cacao (*Theobroma cacao*). (A) Floral landmarks viewed from the side. Scale bar = 5 mm. (B) Petal side door (PSD) and pollinator landmarks. (C) Floral landmarks viewed from above. Blue points (light blue and dark teal) were used for geometric morphometric analysis ($N = 135$). In (B, top), the floral landmarks shown in dark teal ($n = 55$) represent our hypothesized bottleneck to cacao pollination, the petal side door, consisting of sliding landmarks from the left/right petal perimeters (LP, RP) and the abaxial filament length (AF). In (B, bottom), the insect landmarks used for the downstream comparison with petal side door dimensions are shown (Table 2). (C) Points shown in yellow were used to take floral measurements ($N = 25$; Table 1) for comparison with the cacao morphometrics efforts in the literature. Scale bar = 2.5 mm. Surface renderings were visualized in 3D Slicer version 5.0.3 (Kikinis et al., 2014).

Dimensions of hypothesized pollinators versus floral dimensions

Landmarks for the petal side door dimensions were taken from the specimen whose shape was closest to the mean reference specimen (determined using geomorph findMeanSpec) and imported into the 3D Slicer Markups Module. In addition to being the main bottleneck for pollinator access to anthers, the petal side door is also the only portion of the flower that does not change shape or position throughout the pollination phase of anthesis, allowing us to minimize variation between flowers picked at different stages of opening. Three different cross sections of the opening to the petal side door were measured. For comparison with the petal side door dimensions, insect length (longest length from head to tip of abdomen), width (widest body segment when viewed from above), thorax height (at first leg pair), and total height (length of all leg segments + thorax) were measured for all specimens ($N = 10$; one individual per taxon), with a combination of fixed ($N = 6$; for length, width, and thorax height) and sliding semilandmarks ($N = 7-12$ for height, depending on the number of leg segments) following recommendations made by Tatsuta et al. (2018) applied with the 3D Slicer Markups module (Figure 2B). If all dimensions of the insect were smaller than the petal side door dimensions, the insect was marked “likely” as a functionally viable pollinator. If one dimension of the insect was larger than

the petal side door, the insect was marked “possible,” and if two or more dimensions were larger, the insect was marked “unlikely” as a functionally viable pollinator.

To give additional clues on pollinator behavior, floral 3D data sets were investigated for pollinator reward structures, whose presence and location(s) have been controversial (see, for example, Young et al. [1984] and Young [1985], who described their presence, and Vogel [2000], who described their absence). Two whole flowers and one petal were critical point dried with liquid carbon dioxide using a Samdri 780A critical point dryer (Tousimis Research, Rockville, Maryland, USA). They were then mounted to aluminum mounting stubs using a carbon adhesive tab and sputter-coated with approximately 70 nm of gold/palladium with a Denton IV sputter coater (Denton Vacuum, Moorestown, New Jersey, USA). Micrographs were captured using a Phenom XL G2 Desktop scanning electron microscope (SEM) (Thermo Fisher Scientific, Waltham, Massachusetts, USA) at FDACS-DPI.

RESULTS

Micro-CT scanning

Using micro-CT scanning, we generated the first anatomically accurate 3D images of cacao flowers and hypothesized

pollinators with resolutions as low as 6 μm for whole flowers, 1.7 μm for floral closeups, and 1.5 μm for whole insects (Appendix S2). We obtained 68 floral CT data sets, of which 53 were of whole flowers, five were closeups on structures of interest, and 10 were of whole flowers used only to optimize the CT scanning procedures. Of the whole-flower scans for analysis, 40 data sets were retained after the exclusion criteria were applied and subsequently used for the GMM analysis. We also obtained 10 insect CT data sets for comparison with the hypothesized pollinator paths (Appendix S2). The archived CT data sets are available from MorphoSource (see Data Availability Statement).

Floral GMM analysis

We present a modern 3D update to cacao's floral morphology in Figure 3. We show traditional perspectives of the whole flower (Figure 3A, B), androecium (Figure 3C, I, J), gynoecium (Figure 3K–M), and petal hoods (Figure 3G), but also leverage 3D imaging to add new perspectives to the image plate. We show the petal hood with anthers in situ, to highlight how hidden these structures are unless viewed from the base of the petal hood (Figure 3H). We illustrate the three stages of staminal cage anthesis—converging, parallel, and splay (Figure 3D–F)—and show a ceratopogonid midge for reference (Figure 3N). To fully capture floral shape in these unusual flowers, select interactive 3D models are also available from SketchFab (<https://sketchfab.com/katiewolcott/collections/3d-pollination-biology-of-cacao-747c17416efb4a50bdc43d16f4305caf>).

In Table 1, we report the floral morphology measurements of structures commonly studied in cacao for comparison with the literature. The stigma to staminode distance was the most variable trait measured (relative standard deviation [RSD] = 0.38), followed by ovary length and width (RSD = 0.26 and 0.24, respectively). Of structures included for downstream GMM analysis, ligule length and filament length (top) were the most variable (RSD = 0.17 and 0.18, respectively), but all remaining traits were relatively conserved (RSD \leq 0.12). The raw landmark coordinates are provided in Appendix S4.

Our morphospace PCA quantifies the shape variation between flowers, with polygons representing the individual trees sampled (Figure 4). All specimens were included in our morphospace analysis after identifying no outliers in Appendix S5. Principal component 1 (PC1) represents 35.83% of the variation between the floral structures, while PC2 represents 24.19% of the variation. The flowers from all trees overlapped in the morphospace, with trees 2002-120A, 2002-120C, 2009-0862A, CCN-51, and SHRS-7 being the most similar. Flowers from tree 2009-0862 from FTG had the greatest range of variation (shown as a green polygon), while tree 2020-0051 from FTG (shown as a blue polygon) had the least range of variation among its own flowers, but the greatest difference relative to the other trees (note the minimal overlap with other tree polygons). Through our

one-way Procrustes ANOVA, flower size ($F_{1,39} = 5.686$, $P = 0.001$), tree self-compatibility ($F_{1,39} = 4.463$, $P = 0.001$), and tree individual ($F_{4,39} = 1.790$, $P = 0.045$) were statistically significant predictors of floral shape, while collection month was not ($F_{2,39} = 1.774$, $P = 0.071$; Appendix S6).

Dimensions of hypothesized pollinators versus floral dimensions

The petal side door provides the only access to cacao's concealed anthers (Figures 2B, 5A). For the mean reference specimen, we identified the petal side door dimensions to be $2.25 \times 2.37 \times 1.98$ mm across (Figure 5A), which we compared to dimensions of hypothesized pollinators (Table 2; see images in Figure 5). We found that the putative pollinators *Megaselia* sp. (Phoridae, Phoroidea; Figure 5D) and *Sparasion* sp. (Sparasionidae, Platygastridae; Figure 5K) are too large in two dimensions to fit inside the petal hood and access pollen-bearing anthers, qualifying them as unlikely candidate pollinators. The hypothesized pollinators Ceratopogonidae (Chironomoidea; Figure 5B), *Bradysia coprophila* (Siaridae, Siaroidea; Figure 5C), Chloropidae (Carnoidea; Figure 5G), *Crematogaster* sp. (Formicidae, Formicoidea; Figure 5H), and *Calotelea* sp. (Scelionidae, Platygastridae; Figure 5I) are too large in one dimension to access the anthers, classifying them as possible candidate pollinators. Finally, we found that the hypothesized pollinators *Forcipomyia* sp. (Chironomoidea, Ceratopogonidae; Figure 5E) and Thysanoptera (Figure 5J) fit within all dimensions of the petal side door, suggesting they are functionally likely candidate pollinators based on congruence with probable access geometries. We also identified possible floral rewards or pollinator-attracting structures in the form of glandular hairs along the ovary, sepals, and basal staminode surfaces (Figure 6).

DISCUSSION

High-resolution micro-CT imaging allowed us to recover cacao's complex 3D floral structures with unparalleled precision when compared with traditional two-dimensional photographs and illustrations (Figure 3), and to compare their dimensions with cacao's suspected pollinators (Figure 5, Table 2). Three-dimensional GMM enabled us to quantify 3D curved structures using sliding semilandmarks, in addition to applying traditional fixed landmarks on structures relevant for pollination (Figure 2, Table 1). Rather than applying landmarks across all five units of a single flower, the selection of one unit of floral symmetry (one adjacent petal, sepal, carpel, and staminode per flower) enabled us to increase the sample size and efficiency, while still capturing the floral variation between and within trees (Figure 4, Appendix S6). Moreover, our approach does not require symmetry correction, which can be cumbersome for flowers with multiple complex planes of symmetry. Without

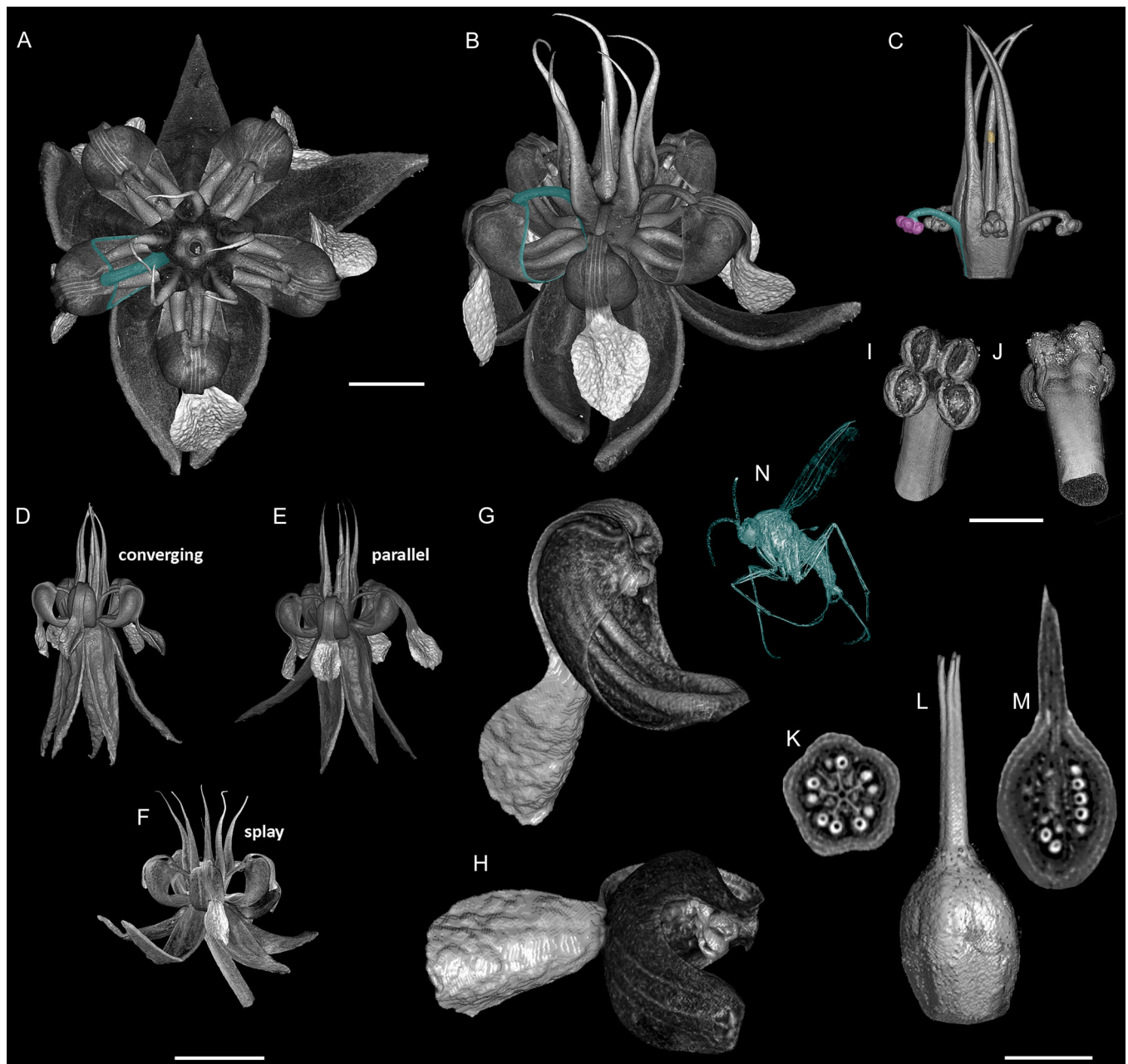


FIGURE 3 Floral morphology of cacao (*Theobroma cacao*) (A–M) and a reference candidate pollinator (N). (A, B) Overall floral morphology from above and side views with petal side door dimensions highlighted in dark teal. (C) Androecium of five fused pairs of stamens with dithecate anthers and five staminodes, all of which are fused at the base to form the staminal tube. To clarify the relevant locations for successful pollination, the anther (location of pollen) is highlighted in magenta, the filament (portion of the petal side door) is shown in dark teal, and the stigma (location for pollen deposition) is in yellow. Scale bar (A–C) = 2 mm. (D–F) Different levels of staminode closure observed during anthesis. Scale bar = 5 mm. (G, H) Petal sac with concealed anthers. Scale bar = 1 mm. (I, J) Anthers, dehiscent with pollen grains. Scale bar = 0.5 mm. (K–M) Gynoecium. Scale bar = 1 mm. Volume renderings of segmentation masked micro-CT data sets visualized in 3D Slicer version 5.0.3 (Kikinis et al., 2014).

multiple units of symmetry, however, we were not able to measure the mean dimensions per flower, nor quantify the measurement error following the methods described by Savriama (2018).

Our micro-CT data sets represent cyberspecimens (Favret, 2014) that provide high-resolution internal and external anatomies of cacao flowers for future study and are deposited in MorphoSource, with select models available on

Sketchfab.com (see Data Availability Statement). This archive is available for future use in modern morphological and evolutionary studies that would benefit from having high-resolution internal 3D anatomy, such as comparing volumes or areas. For instance, in taxa with very small flowers and large fruits, such as cacao and other species within *Theobroma* L., micro-CT data sets present an opportunity for identifying the lower developmental limits

TABLE 1 Summary of morphology measurements (in millimeters) for 40 cacao flowers derived from the landmarks in Figure 2. The first four rows of measurements are shown with yellow dots in Figure 2C and were not used in the geometric morphometric (GMM) analyses. The remaining nine were also used in the downstream GMM analyses and are shown as blue dots in Figure 2A, B. The measurements were obtained using the Markups Module in 3D Slicer version 5.0.3 (Kikinis et al., 2014) and analyzed using native functions in R (R Core Team, 2021).

Floral trait	Minimum	Median	Maximum	SD	RSD
Ovary length	0.77	1.16	2.43	0.30	0.26
Ovary width	1.09	1.40	2.80	0.35	0.24
Style length	1.39	2.14	3.28	0.33	0.15
Stigma to staminode distance	0.00	0.98	1.71	0.36	0.38
Staminode tube length	1.40	1.70	2.16	0.17	0.10
Filament length (top)	1.71	2.31	3.38	0.41	0.17
Filament length (bottom)	2.36	2.85	4.13	0.35	0.12
Ligule length	5.44	6.34	8.06	0.62	0.10
Ligule width	1.58	2.15	3.39	0.39	0.18
Sepal length	6.77	8.07	9.56	0.60	0.07
Sepal width	1.68	2.17	2.73	0.26	0.12
Petal curve (right)	3.03	3.66	4.85	0.47	0.12
Petal curve (left)	3.16	3.83	4.94	0.47	0.12

Note: RSD = relative standard deviation; SD = standard deviation.

on the ratio of ovary size to fruit size. Staedler et al. (2018) used a similar approach with micro-CT to quantify the reproductive investment for orchid flowers with deceptive and rewarding strategies. Micro-CT and 3D GMM can also be used to quantify other internal microanatomies, such as the ovule number, pollen volume, and tissue density, with much more precision and ease than traditional serial sectioning and histology.

The time investment needed for morphological analyses using micro-CT would be greatly reduced by improving existing methods for automated landmark placement, permitting larger and more representative sample sizes. We attempted using automated semilandmark placement with ALPACA (Porto et al., 2021), PseudoLMGenerator (Rolfe et al., 2021), and auto3dgm (Boyer et al., 2015) in 3D Slicer; however, all methods failed to capture the complexity of cacao's flowers and recover the spatial variation in their soft tissue structures, especially when any of these individual repeating structures were missing. These tools were primarily developed for use with vertebrate specimens, whose ossified structures have minimal positional variation. None of the mentioned automated landmarking tools consider rotational symmetry, which is commonly found in plants (e.g., Savriama, 2018). We propose incorporating options to account for rotational symmetry in automated

landmarking tools to facilitate 3D GMM with complex plant morphologies. Furthermore, supplementing large micro-CT data sets of internal anatomy with smaller photogrammetry data sets of external morphology would facilitate collection of larger sample sizes at a faster pace, reduced cost, and without necessitating the export of specimens from field location to imaging facilities (James et al., 2023; Leménager et al., 2023). Field-based photogrammetry approaches have been shown to achieve comparable 3D model accuracy for flowers as small as 2 cm using a standard digital single-lens reflex (DSLR) camera and a fixed focal-length macro lens (Leménager et al., 2023).

Our focal species, *Theobroma cacao*, is especially well suited for 3D image analysis due to its intricate morphology separating the anthers from the stigma (Figure 3A, B, G, H). Here, we found that the flowers of all sampled trees in South Florida had overlapping floral variation in the morphospace, but two trees stood out (Figure 4); tree 2009-0862 from FTG showed the greatest range of variation, while tree 2020-0051 from FTG showed the least variation. The former is growing inside a greenhouse and is older, whereas the latter is younger and growing outdoors in a drier microhabitat. For cacao, it is not known whether variation in floral morphology has an ontogenetic component, environmental plasticity, or if genetics plays a role. Floral morphology and development have been documented to change in response to climatic variables for some species (Gray and Brady, 2016; Weber et al., 2020), and the recorded differential impacts on various important crops highlights the need for an investigation into the specific changes that may occur in cacao (Tripathi et al., 2016).

Through a one-way Procrustes ANOVA, we determined that flower size, self-compatibility, and tree individual were significant predictors of floral shape (Appendix S6). Future studies that include trees from known genetic groups of cacao (Motamayor et al., 2008; Zhang et al., 2009; Fouet et al., 2022) could be used to identify heritable differences in floral shape. Cacao self-compatibility has been attributed to a late gameto-sporophytic system (Knight and Rogers, 1955; Cope, 1958; Royaert et al., 2011; Lanaud et al., 2017), but to the best of our knowledge, no relationship between floral morphology and self-compatibility has yet been identified. As self-compatibility is measured at the level of the tree individual, it was not possible to disentangle confounding effects of either variable on floral morphology using our ANOVA. Whether the morphological differences we found can be attributed to self-compatibility, tree individual, or result from other factors (for instance, population bottlenecks experienced by plants in living collections) also merits further study. Particularly interesting would be the identification of changes in floral morphology that are associated with domesticated populations (Cornejo et al., 2018).

Our method using geometry to narrow the candidate search for putative pollinators has allowed us to predict the greatest bottleneck for pollinator access to cacao's deeply concealed anthers—the petal side door. Previous studies often cited 3 mm as the upper size threshold for cacao's

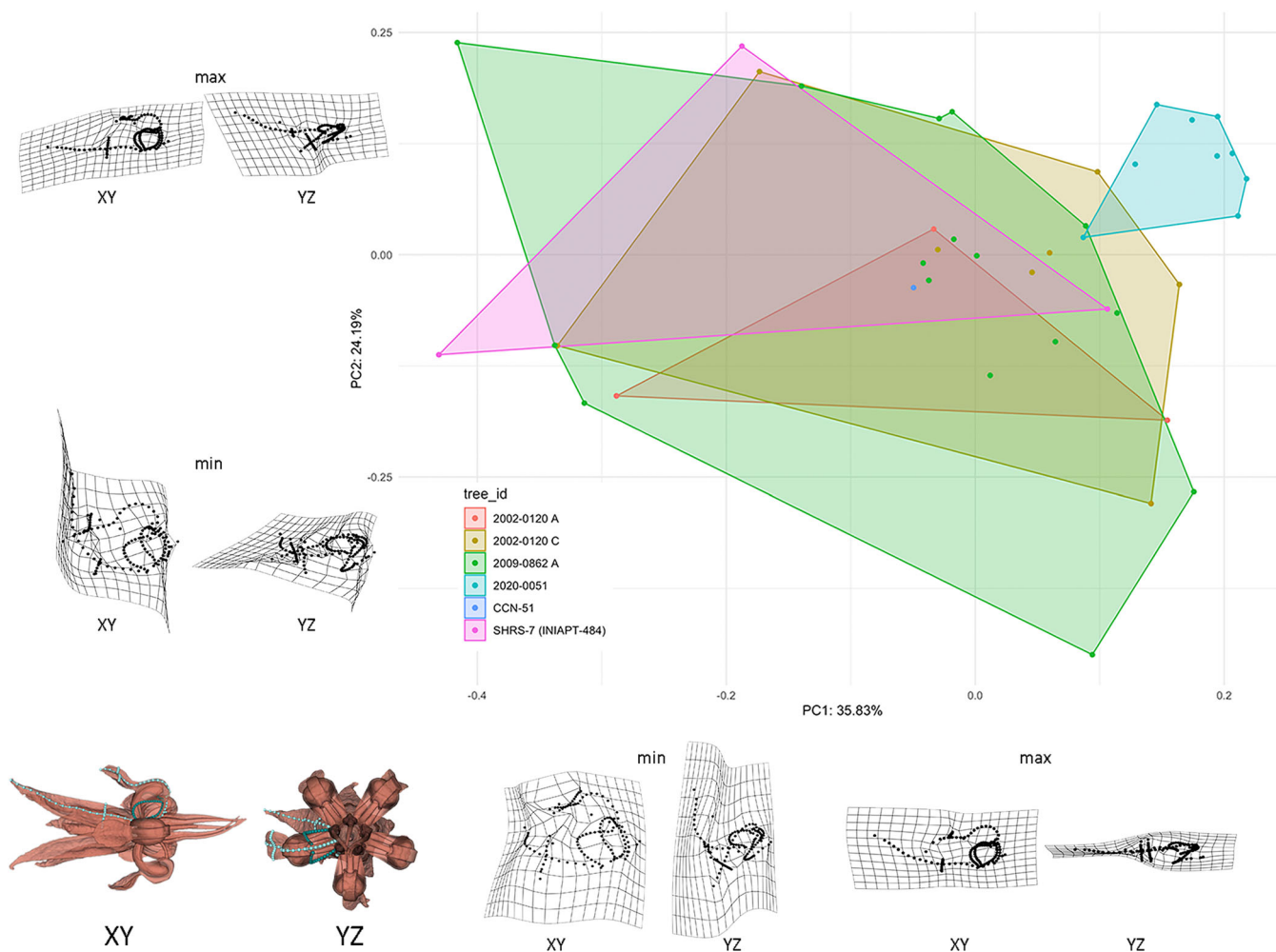


FIGURE 4 Morphospace analysis of cacao flowers (*Theobroma cacao*; $N = 40$) using fixed and sliding semilandmarks ($N = 135$) applied to one adjacent petal, ligule, sepal, and staminode per flower (shown as blue dots on XY and YZ surface models, bottom left). Thin-plate-spline (TPS) deformation grids show differences between the minimum/maximum and mean shape along principal components (PC)1 and 2. Maximum shapes for PC1 and PC2 show minimal differences when compared with the mean, while minimum shapes show considerable differences and grid deformation. Polygons are minimum convex hulls for each tree sampled. PC1 represents 35.83% of the variance between floral structures and PC2 represents 24.19%. Flowers from all trees overlapped in morphospace, but tree 2020-0051 (shown in blue) shares the least overlap with the other individuals. Tree 2009-0862A (green) showed the widest range of variation. Figure generated using geomorph version 4.0.5 (Adams and Otárola-Castillo, 2013), ggplot2 (Wickham, 2016) in R version 4.0.5 (R Core Team, 2021), and Adobe Photoshop version 23.2.

pollinators based on floral visitor surveys (Young, 1985; Toledo-Hernández et al., 2017); however, we measured three cross sections of the petal side door for the mean consensus flower reconstruction from our GMM analysis and found that the petal side door widths are $2.25 \times 2.37 \times 1.98$ mm (Figure 5A). Such an observation suggests that the likely candidate pollinators are smaller insects than previously believed. Based on our dimensional analysis of the petal side door, we determined three levels of access likelihood: most likely (pollinator candidate fits in all dimensions), possible (pollinator candidate does not fit in one dimension), and unlikely (pollinator candidate does not fit in two dimensions).

Under this classification system for spatial access, one ceratopogonid midge (*Forcipomyia* sp.; Figure 5E, Table 2), which is often cited as cacao's most likely pollinator, was

predicted to be a likely candidate, as it was able to fit within all petal side door dimensions. Another ceratopogonid (Figure 5B) was classified as a possible pollinator because it was too large in one dimension (height) to fit through the petal side door. Thrips (Thysanoptera; Figure 5H), which are commonly considered agricultural pests (Entwistle, 1972), were also classified as a likely candidate. Platygastridae are a commonly cited candidate pollinator taxon, and two platygastriid wasps (*Macroteleia* sp. and *Calotelia* sp.; Figures 5F and 5I) were classified as possible pollinators, while another (*Sparasion* sp.; Figure 5K) was classified as an unlikely pollinator. We measured insect height as the length of a fully extended leg (via the sum of all segments) plus the height of the thorax. As a result, our size metric does not take into account insect height during movement through the flowers and is likely a conservative estimate; for

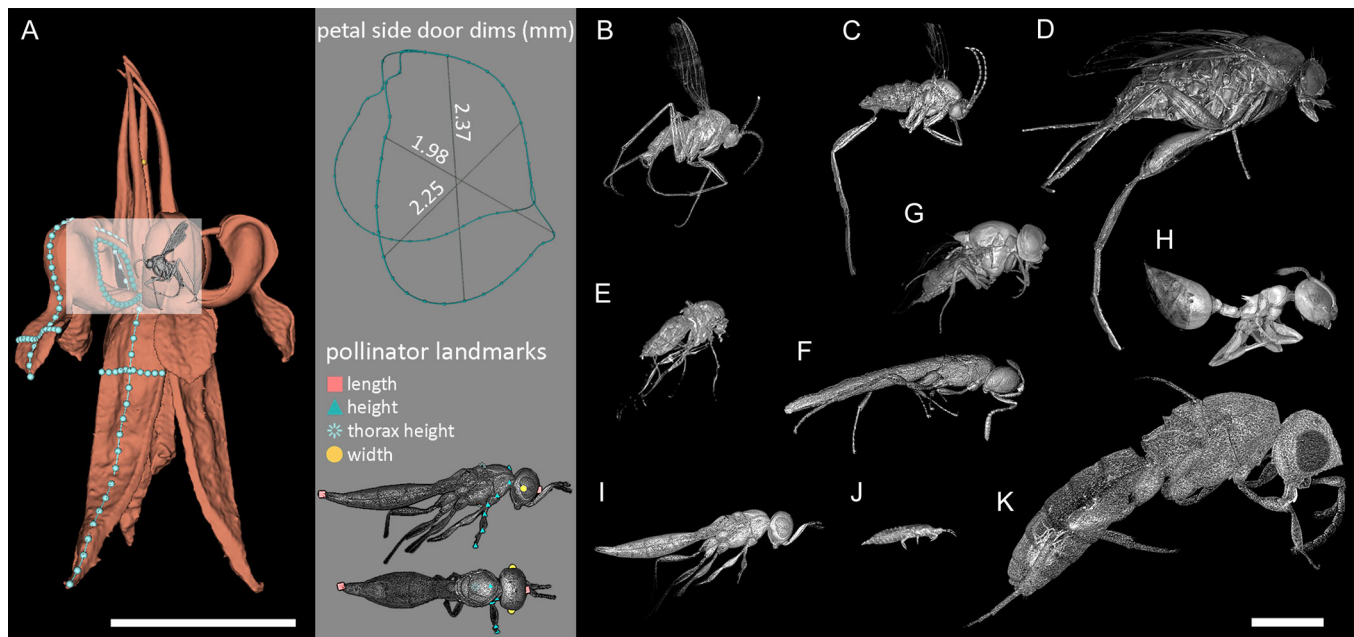


FIGURE 5 Petal side door dimensions and corresponding pollinator landmarks used to evaluate the fit for hypothesized pollinator taxa. (A) Petal side door dimensions and corresponding pollinator landmarks. Scale bar = 5 mm. (B–K) Hypothesized pollinator taxa, including Diptera (B–E, G), Hymenoptera (F, H, I, K), and Thysanoptera (J). Scale bar = 1 mm. Insect measurements and lower-level taxonomic classifications are shown in Table 2. Using our metric for pollinator access, insects E and J were classified as most likely functional pollinators (fit in all dimensions); B, C, and F–I were classified as possible (too large in one dimension); and D and K were classified as unlikely (too large in two dimensions).

example, if the thorax and head fit into the petal hood, but not the extended legs and full body length, it is still possible that an insect could access pollen. Nonetheless, our functional approach to 3D pollination biology allowed us to narrow the list of putative pollinators from the literature, giving clues for future studies to further analyze pollinator behavior in these flowers and the most relevant bodily positions to measure.

To more accurately predict the viability of candidate pollinators, geometry should be incorporated as a factor in predictive models that consider floral and pollinator traits (e.g., Garibaldi et al., 2015; Rico-Guevara et al., 2021; reviewed by Dellinger, 2020). While our metric only considers the upper size limit of a functionally viable pollinator and their corresponding restrictions to access anthers, the factors that may influence the lower size limits are unknown; for example, 115 grains of pollen are suspected to be needed for successful pollination in cacao (Falque et al., 1995), but field experiments have reported lower values for cacao's most frequent floral visitors (Vansynghel et al., 2022). In addition to pollinator size, the relative hairiness of the insect body may limit their ability to carry pollen, both of which merit further study (Young, 1985). Pollinator behavior may also influence their ability to deposit pollen on the stigma when walking along staminodes, particularly if they are too small to come into contact with the stigma (e.g., Frimpong-Anin et al., 2014).

In addition to geometry, floral rewards will likely provide additional clues for predictive pollinator modeling

efforts, as different pollinator reward locations and types are associated with specific taxa (e.g., Simpson and Neff, 1981; Young et al., 1984; Frimpong et al., 2009; Verstraete et al., 2014). The glandular hairs identified using high-resolution 3D imaging (Figure 6) add evidence to previously conflicting arguments about floral rewards in cacao, supporting studies that described their presence (Young et al., 1984; Young, 1985). These structures are prime candidates for performing a localized analysis (e.g., mass spectroscopy on dissected glands) to determine the anatomical structures that may be releasing aromatic compounds. Other ecological and behavioral elements should also be considered. Visual cues based on candidate pollinator visual systems would provide additional information on sensory signaling from plants to potential pollinators (e.g., UV markings or polarized light for expected fly pollinators; Young et al., 1987; Whitney et al., 2009; Lunau, 2014; van der Kooij et al., 2019; Hardcastle et al., 2021). Camera traps are a useful tool for observing pollinator behavior, but currently published setups are only effective for larger insects, such as honeybees, butterflies, and ladybugs (e.g., Pegoraro et al., 2020; Droissart et al., 2021; Bjerger et al., 2022). Refining camera traps for small insects (≤ 3 mm) would further enhance efforts to study cacao pollination.

With pollinator declines and climate change, creative approaches to find candidate pollinators for the world's crops are needed to protect global food security (Klein et al., 2007; Reilly et al., 2020). Cacao is a culturally important pre-Columbian crop with over 5000 years of cultivation in the tropical Americas (Zarrillo et al., 2018). Knowledge from

TABLE 2 Dimensions of hypothesized pollinators ($N = 10$) compared with the petal side door illustrated in Figure 5A with mean dimensions of $2.25 \times 2.37 \times 1.98$ mm across. Using these petal side door dimensions, we determined three levels of access likelihood for pollinators to be functionally viable candidates: most likely (pollinator candidate fits in all dimensions), possible (pollinator candidate does not fit in one dimension), and unlikely (pollinator candidate does not fit in two dimensions). Insect body dimensions are shown.

ID ^a	Order	Superfamily	Family	Genus/Species ^b	L	W	Htl	Ht	Pollinator likelihood	Catalog number
B	Diptera	Chironomoidea	Ceratopogonidae	—	1.42	0.46	2.72	0.41	possible	CERSPP_MOC_LKSP_C_2022-09-21
C	Diptera	Sciaroidea	Sciaridae	<i>Bradysia coprophila</i> Lintner, 1895	1.51	0.40	3.57	0.50	possible	BRACOP_MC_BRA_C_1985-02-07
D	Diptera	Phoroidea	Phoridae	<i>Megaselia Rondani</i> , 1856	3.21	0.98	5.83	0.75	unlikely	MEGSPP_AC_RC_B_1956-12-16
E	Diptera	Chironomoidea	Ceratopogonidae	<i>Forcipomyia Meigen</i> , 1818	1.33	0.45	1.51	0.59	most likely	FORSPP_MOC_V_C_2022-10-xx
F	Hymenoptera	Platygastroidea	Scelionidae	<i>Macroteleia Westwood</i> , 1835	3.41	0.539	2.28	0.49	possible	MACSPP_USDA_MIA_T32_2019-03-04
G	Diptera	Carnoidea	Chloropidae	—	2.21	0.77	2.39	0.60	possible	CHLSPP_OC_PH_D_1972-01-31
H	Hymenoptera	Formicoidea	Formicidae	<i>Crematogaster Lund</i> , 1831	2.73	0.45	2.29	0.48	possible	CRESPP_BI_POJ_T25_2020-10-20
I	Hymenoptera	Platygastroidea	Scelionidae	<i>Calotelea Westwood</i> , 1837	3.20	0.54	1.37	0.48	possible	CALSPP_SC_WS_T22_2021-03-14
J	Thysanoptera	—	—	—	1.13	0.27	0.46	0.16	most likely	THYSPP_GNV_TJW_Th_2017-04-05
K	Hymenoptera	Platygastroidea	Sparasionidae	<i>Sparasion Latreille</i> , 1802	4.96	1.41	4.33	1.00	unlikely	SPASPP_AC_HPSP_T11_2022-06-05

Note: Ht = height of insect thorax; Htl = height of insect thorax and leg; L = insect body length; W = insect body width.

^aID corresponds to the insect images in Figure 5B–K.

^bGenus/species provided when available.

indigenous peoples and local communities from these regions is an invaluable resource that may guide the identification of candidate pollinators and development of sustainable agroforestry practices outside its native range (Forbes and Northfield, 2017; Hill et al., 2019; Franco-Moraes et al., 2021; Wanger et al., 2021). While cacao's importance makes it an ideal study system to refine pollinator prediction models, our methods for incorporating 3D GMM and micro-CT to study candidate pollinators are applicable to any plant with restricted access to anthers, stigma, or floral rewards; for example, any of the other ~21 species with concealed anthers in the Byttnerioideae, such as those found within *Herrania* Goudot, *Guazuma* Mill., *Abroma* Jacq., *Scaphopetalum* Mast., *Byttneria* Loefl., and *Ayenia* L. (Whitlock et al., 2001), as well as genera from other families, such as *Ceropegia* L. (Apocynaceae),

Aristolochia L. (Aristolochiaceae), and *Sarracenia* L. (Sarraceniaceae).

Many questions remain about pollination in cacao. Our method using micro-CT imaging and 3D GMM provided clues toward the identity of cacao's effective pollinators, but combining this data with existing trait matching models of plant–pollinator syndromes (reviewed by Dellinger, 2020) would provide the strongest support for predicted pollinator taxa. Our methods would benefit from incorporating 3D data sets from known cacao cultivars and wild varieties, supplemented by behavioral data from camera traps and the identification of compounds produced by the glandular trichomes we identified on the ovary. Additionally, investigating the factors determining the lower size limits of an effective pollinator would give a narrower geometric definition of a functionally viable candidate pollinator. In

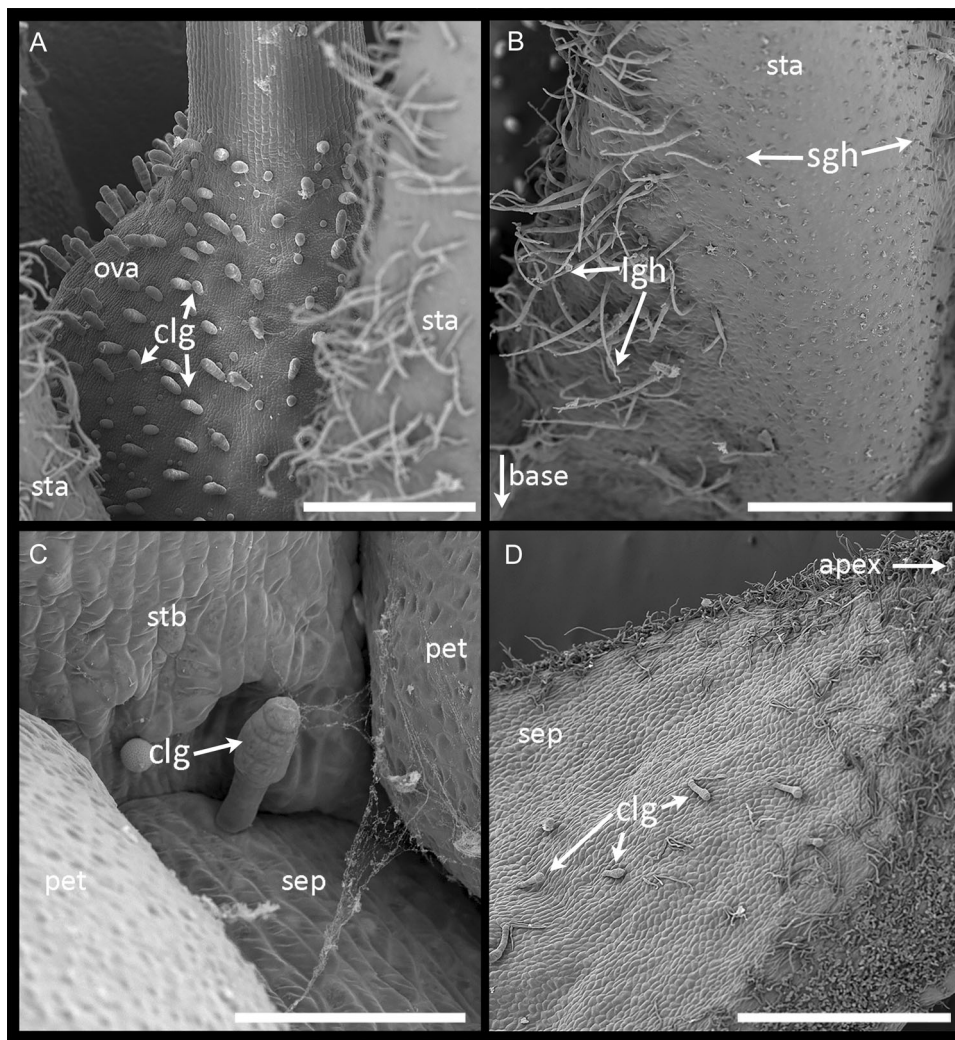


FIGURE 6 Possible floral reward or pollinator-attracting structures in cacao flowers (*Theobroma cacao*). (A–D) Structures on (A) ovary, (B) the lower two-thirds of the staminode adaxial surface, and (C, D) the sepal adaxial surfaces between two petals near the point of insertion (C) and near the sepal apex (D). clg = club-like glandular hair; lgh = long glandular hair; ova = ovary; pet = petal; sep = sepal; sgh = short glandular hair; sta = staminode; stb = staminal tube. Scale bars = 0.3 mm (A, B), 0.1 mm (C), and 0.5 mm (D). Structure classification follows terms used by Young et al. (1984). Images captured using a Phenom XL G2 Desktop scanning electron microscope.

the face of global insect declines and climate change, pollination biology studies leveraging 3D functional morphology will become increasingly important. Using micro-CT and 3D GMM for flowers and their pollinators elucidates the positional relationships of structures in situ at high resolution, is reproducible, and creates valuable cyberspecimens that can be reused for comparative analyses of large-scale biodiversity trends that were not feasible with traditional morphometrics methods from only a few years ago.

AUTHOR CONTRIBUTIONS

B.A.W., S.W., and K.A.W. planned and designed the research. B.A.W., O.A.G., and K.A.W. surveyed the collecting localities and collected specimens. B.A.W. and O.A.G. offered their expertise on cacao for the study design and interpretation. K.A.W. and E.L.S. carried out the

specimen preparation, micro-CT scanning, and troubleshooting. K.A.W. and S.W. analyzed the data with the support of the other authors. All authors wrote the first draft and approved the final version of the manuscript.

ACKNOWLEDGMENTS

The authors thank the University of Miami Fellowship for funding K.A.W.'s graduate stipend. For financing research-related costs and travel, we thank the University of Miami Biology Department Graduate Student Research Awards (Evoy Fund, Kushlan Fund, Cross Lab Award), the Graduate Activity Fee Allocation Committee, the Christiane Tyson Research Fund, the Botanical Society of America Bill Dahl Graduate Student Research Grant, the Tropical Fern and Exotic Plant Society Student Scholarship, and the Society for Integrative and Comparative Biology Fellowship of Graduate Student Travel. Gary Scheffele and Kristy

Schepker at the University of Florida Nanoscale Research Facility provided assistance when using the ZEISS Versa 620 XRM (purchased under a National Science Foundation [NSF] Division of Materials Research Grant [#2017977]). Ali Ghahremaninezhad and Sadeh Tale at the University of Miami Advanced Infrastructure Materials Research Laboratory assisted our use of the Bruker Skyscan 1273 (purchased under a NSF Major Research Instrumentation Program Grant [#1920127]). Brett Jestrow at Fairchild Tropical Botanic Garden provided support regarding our collection of the flower specimens. Steven Wagner and Wil Quintanilla at the Subtropical Horticultural Research Station, USDA-ARS (Miami, Florida, USA), helped us to set up the camera traps. Erick Rodriguez, Gary Steck, Bill Grogan, Jonathan Bremen, and Elijah Talamas at Florida Department of Agriculture and Consumer Sciences Division of Plant Industry loaned and gifted insect specimens for study, and Jonathan Bremen assisted our generation of SEM images. Larry Hribar at Keys Mosquito Control gifted us midges for study. Susanne Renner at Washington University provided us with a hard copy of Vogel (2000). We are also grateful to Laís Lautenschlager Rodrigues and Yuri Silva De Souza at University of Miami for translating the abstract into Portuguese; William Browne at University of Miami for proofreading; and two anonymous reviewers, *Applications in Plant Sciences* Associate Editor Luiza Teixeira-Costa, copyeditor Sarah Jose, and managing editor Beth Parada for their suggestions that greatly improved the manuscript.

OPEN RESEARCH BADGES



This article has earned Open Data and Open Materials badges. Data and materials are available at <https://www.morphosource.org/projects/000461839>, https://github.com/aubricot/Cacao_3D_gmm.

DATA AVAILABILITY STATEMENT

The processing and analysis pipelines used here are open source and available from GitHub, along with the landmark files (https://github.com/aubricot/Cacao_3D_gmm). The CT data sets are available from MorphoSource (<https://www.morphosource.org/projects/000461839>). Select 3D models for outreach and/or easy visualization are available from Sketchfab (<https://sketchfab.com/katiewolcott/collections/3d-pollination-biology-of-cacao-747c17416efb4a50bdc43d16f4305caf>).

ORCID

Katherine A. Wolcott <http://orcid.org/0000-0002-6025-4569>

Edward L. Stanley <http://orcid.org/0000-0001-5257-037X>

Osman A. Gutierrez <http://orcid.org/0000-0002-7278-1067>

Stefan Wuchty <http://orcid.org/0000-0001-8916-6522>

Barbara Ann Whitlock <http://orcid.org/0000-0002-6976-1866>

REFERENCES

- Adams, D. C., and E. Otárola-Castillo. 2013. Geomorph: An R package for the collection and analysis of geometric morphometric shape data. *Methods in Ecology and Evolution* 4: 393–399.
- Alves, R. M., A. A. F. Garcia, E. D. Cruz, and A. Figueira. 2003. Seleção de descritores botânico-agronômicos para caracterização de germoplasma de cupuaçuzeiro. *Pesquisa Agropecuária Brasileira* 38: 807–818.
- Arnold, S. E. J., S. J. Forbes, D. R. Hall, D. I. Farman, P. Bridgemohan, G. R. Spinelli, D. P. Bray, et al. 2019. Floral odors and the interaction between pollinating ceratopogonid midges and cacao. *Journal of Chemical Ecology* 45: 869–878.
- Bayer, C., and J. Hoppe. 1990. Die blütenentwicklung von *Theobroma cacao* L. (Sterculiaceae). *Beiträge zur Biologie der Pflanzen* 65: 301–312.
- Bekele, F. L., I. Bekele, D. R. Butler, and G. G. Bidaisee. 2006. Patterns of morphological variation in a sample of cacao (*Theobroma cacao* L.) germplasm from the International Cocoa Genebank, Trinidad. *Genetic Resources and Crop Evolution* 53: 933–948.
- Bilbao, G., A. Bruneau, and S. Joly. 2021. Judge it by its shape: A pollinator-blind approach reveals convergence in petal shape and infers pollination modes in the genus *Erythrina*. *American Journal of Botany* 108: 1716–1730.
- Bjerger, K., H. M. R. Mann, and T. T. Høye. 2022. Real-time insect tracking and monitoring with computer vision and deep learning. *Remote Sensing in Ecology and Conservation* 8: 315–327.
- Boyer, D. M., J. Puente, J. T. Gladman, C. Glynn, S. Mukherjee, G. S. Yapuncich, and I. Daubechies. 2015. A new fully automated approach for aligning and comparing shapes. *Anatomical Record* 298: 249–276.
- Chumacero de Schawe, C., M. Kessler, I. Hensen, and T. Tschardtke. 2018. Abundance and diversity of flower visitors on wild and cultivated cacao (*Theobroma cacao* L.) in Bolivia. *Agroforestry Systems* 92: 117–125.
- Cope, F. W. 1958. Incompatibility in *Theobroma cacao*. *Nature* 181: 279.
- Cornejo, O. E., M. C. Yee, V. Dominguez, M. Andrews, A. Sockell, E. Strandberg, D. Livingstone, et al. 2018. Population genomic analyses of the chocolate tree, *Theobroma cacao* L., provide insights into its domestication process. *Communications Biology* 1: 167.
- Cuatrecasas, J. 1964. Cacao and its allies. A taxonomic revision of the genus *Theobroma*. *National Herbarium* 35: 379–607.
- Dellinger, A. S. 2020. Pollination syndromes in the 21st century: Where do we stand and where may we go? *New Phytologist* 228: 1193–1213.
- Dellinger, A. S., D. S. Penneys, Y. M. Staedler, L. Fragner, W. Weckwerth, and J. Schönenberger. 2014. A specialized bird pollination system with a bellows mechanism for pollen transfer and staminal food body rewards. *Current Biology* 24: 1615–1619.
- Dellinger, A. S., S. Artuso, S. Pamperl, F. A. Michelangeli, D. S. Penneys, D. M. Fernández-Fernández, M. Alvear, et al. 2019. Modularity increases rate of floral evolution and adaptive success for functionally specialized pollination systems. *Communications Biology* 2: 453.
- Droissart, V., L. Azandi, E. R. Onguene, M. Savignac, T. B. Smith, and V. Deblauwe. 2021. PICT: A low-cost, modular, open-source camera trap system to study plant–insect interactions. *Methods in Ecology and Evolution* 12: 1389–1396.
- Engels, J. M. M. 1983. A systematic description of cacao clones. III. Relationships between clones, between characteristics and some consequences for the cacao breeding. *Euphytica* 32: 719–733.
- Entwistle, P. F. 1972. Pests of cocoa. Longmans, London, United Kingdom.
- Erickson, B. J., A. M. Young, M. A. Strand, and E. H. Erickson. 1987. Analyses of floral oils. *Insect Science Applications* 8: 301–310.
- Falque, M., A. Vincent, B. E. Vaissiere, and A. B. Eskes. 1995. Effect of pollination intensity on fruit and seed set in cacao (*Theobroma cacao* L.). *Sexual Plant Reproduction* 8: 354–360.
- FAO (Food and Agriculture Organization of the United Nations). 2023. FAOSTAT statistical database. Website: <https://www.fao.org/faostat/> [accessed 3 February 2023].
- Favret, C. 2014. Cybertaxonomy to accomplish big things in aphid systematics. *Insect Science* 21: 392–399.

- Forbes, S. J., and T. D. Northfield. 2017. Increased pollinator habitat enhances cacao fruit set and predator conservation. *Ecological Applications* 27: 887–899.
- Forbes, S. J., G. Mustiga, A. Romero, T. D. Northfield, S. Lambert, and J. C. Motamayor. 2019. Supplemental and synchronized pollination may increase yield in cacao. *HortScience* 54: 1718–1727.
- Fouet, O., R. G. Loor Solorzano, B. Rhoné, C. Subía, D. Calderón, F. Fernández, I. Sotomayor, et al. 2022. Collection of native *Theobroma cacao* L. accessions from the Ecuadorian Amazon highlights a hotspot of cocoa diversity. *Plants People Planet* 4: 605–617.
- Franco-Moraes, J., C. R. Clement, J. C. de Oliveira, and A. A. de Oliveira. 2021. A framework for identifying and integrating sociocultural and environmental elements of indigenous peoples' and local communities' landscape transformations. *Perspectives in Ecology and Conservation* 19: 143–152.
- Frimpong, E. A., I. Gordon, P. K. Kwabong, and B. Gemmill-Herren. 2009. Dynamics of cocoa pollination: Tools and applications for surveying and monitoring cocoa pollinators. *International Journal of Tropical Insect Science* 29: 62–69.
- Frimpong-Anin, K., M. K. Adjalo, P. K. Kwabong, and W. Oduro. 2014. Structure and stability of cocoa flowers and their response to pollination. *Journal of Botany* 2014: 513623.
- Garibaldi, L. A., I. Bartomeus, R. Bommarco, A. M. Klein, S. A. Cunningham, M. A. Aizen, V. Boreux, et al. 2015. Trait matching of flower visitors and crops predicts fruit set better than trait diversity. *Journal of Applied Ecology* 52: 1436–1444.
- Gonzalez, P. N., J. Barbeito-Andrés, L. A. D'Addona, V. Bernal, and S. I. Perez. 2016. Technical note: Performance of semi and fully automated approaches for registration of 3D surface coordinates in geometric morphometric studies. *American Journal of Physical Anthropology* 160: 169–178.
- Goulson, D. 2019. The insect apocalypse, and why it matters. *Current Biology* 29: R967–R971.
- Gray, S. B., and S. M. Brady. 2016. Plant developmental responses to climate change. *Developmental Biology* 419: 64–77.
- Groeneveld, J. H., T. Tschardt, G. Moser, and Y. Clough. 2010. Experimental evidence for stronger cacao yield limitation by pollination than by plant resources. *Perspectives in Plant Ecology, Evolution and Systematics* 12: 183–191.
- Hardcastle, B. J., J. J. Omoto, P. Kandimalla, B. C. M. Nguyen, M. F. Keleş, N. K. Boyd, V. Hartenstein, and M. A. Frye. 2021. A visual pathway for skylight polarization processing in *Drosophila*. *eLife* 10: e63225.
- Hill, R., G. Nates-Parra, J. J. G. Quezada-Euán, D. Buchori, G. LeBuhn, M. M. Maués, P. L. Pert, et al. 2019. Biocultural approaches to pollinator conservation. *Nature Sustainability* 2: 214–222.
- James, N., A. Adkinson, and A. Mast. 2023. Rapid imaging in the field followed by photogrammetry digitally captures the otherwise lost dimensions of plant specimens. *Applications in Plant Sciences* 11(5): e11547.
- Jaramillo, F., Q. Guerrero, and T. Guncay. 2022. Morfología floral en 20 árboles élite de la colección de Cacao de la Utmach. *Revista Científica Agroecosistemas* 10: 58–64.
- Jürgens, A. 2006. Comparative floral morphometrics in day-flowering, night-flowering and self-pollinated Caryophylloideae (*Agrostemma*, *Dianthus*, *Saponaria*, *Silene*, and *Vaccaria*). *Plant Systematics and Evolution* 257: 233–250.
- Kaufmann, T. 1974. Behavioral biology of a cocoa pollinator, *Forcipomyia inornatipennis* (Diptera: Ceratopogonidae) in Ghana. *Journal of the Kansas Entomological Society* 47: 541–548.
- Keklikoglou, K., S. Faulwetter, E. Chatzinikolaou, P. Wils, J. Brecko, J. Kvaček, B. Metscher, and C. Arvanitidis. 2019. Micro-computed tomography for natural history specimens: a handbook of best practice protocols. *European Journal of Taxonomy* 522: 1–55.
- Kikinis, R., S. D. Pieper, and K. G. Vosburgh. 2014. 3D Slicer: A platform for subject-specific image analysis, visualization and clinical support. In F. Jolesz [ed.], *Intraoperative Imaging and Image-Guided Therapy*, 277–289. Springer, New York, New York, USA.
- Klein, A. M., B. E. Vaissière, J. H. Cane, I. Steffan-Dewenter, S. A. Cunningham, C. Kremen, and T. Tschardt. 2007. Importance of pollinators in changing landscapes for world crops. *Proceedings of the Royal Society B: Biological Sciences* 274: 303–313.
- Knight, R., and H. H. Rogers. 1955. Incompatibility in *Theobroma cacao*. *Heredity* 9: 69–77.
- Kubitzki, K., and C. Bayer. 2003. The Families and Genera of Vascular Plants, Vol. 5: Flowering Plants, Dicotyledons: Malvales, Capparales and Non-betain Caryophyllales. Springer, Berlin, Germany.
- Lanaud, C., O. Fouet, T. Legavre, U. Lopes, O. Sounigo, M. C. Eyango, B. Mermaz, et al. 2017. Deciphering the *Theobroma cacao* self-incompatibility system: From genomics to diagnostic markers for self-compatibility. *Journal of Experimental Botany* 68: 4775–4790.
- Leménager, M., J. Burkiewicz D. J. Schoen, and S. Joly. 2023. Studying flowers in 3D using photogrammetry. *New Phytologist* 237(5): 1922–51933.
- Lunau, K. 2014. Visual ecology of flies with particular reference to colour vision and colour preferences. *Journal of Comparative Physiology A: Neuroethology, Sensory, Neural, and Behavioral Physiology* 200: 497–512.
- Metscher, B. D. 2009. MicroCT for comparative morphology: Simple staining methods allow high-contrast 3D imaging of diverse non-mineralized animal tissues. *BMC Physiology* 9: 11.
- Motamayor, J. C., P. Lachenaud, J. W. da Silva e Mota, R. Loor, D. N. Kuhn, J. S. Brown, R. J. Schnell. 2008. Geographic and genetic population differentiation of the Amazonian chocolate tree (*Theobroma cacao* L.). *PLoS ONE* 3: e3311.
- Pegoraro, L., O. Hidalgo, I. J. Leitch, J. Pellice, and S. E. Barlow. 2020. Automated video monitoring of insect pollinators in the field. *Emerging Topics in Life Sciences* 4: 87–97.
- Porto, A., S. Rolfe, and A. M. Maga. 2021. ALPACA: A fast and accurate computer vision approach for automated landmarking of three-dimensional biological structures. *Methods in Ecology and Evolution* 12: 2129–2144.
- Posnette, A. F. 1950. The pollination of cacao in the Gold Coast. *Journal of Horticultural Science* 25: 155–163.
- R Core Team. 2021. R: A language and environment for statistical computing. R Foundation for Statistical Computing, Vienna, Austria. Website: <https://www.R-project.org/> [accessed 15 September 2023].
- Rakosy, D., M. Cuervo, H. F. Paulus, and M. Ayasse. 2017. Looks matter: Changes in flower form affect pollination effectiveness in a sexually deceptive orchid. *Journal of Evolutionary Biology* 30: 1978–1993.
- Reich, D., A. Berger, M. von Balthazar, M. Chartier, M. Sherafati, J. Schönenberger, S. Manafzadeh, and Y. M. Staedler. 2020. Modularity and evolution of flower shape: The role of function, development, and spandrels in *Erica*. *New Phytologist* 226: 267–280.
- Reilly, J. R., D. R. Artz, D. Biddinger, K. Bobiwash, N. K. Boyle, C. Brittain, J. Brokaw, et al. 2020. Crop production in the USA is frequently limited by a lack of pollinators. *Proceedings of the Royal Society B: Biological Sciences* 287: 2–9.
- Rico-Guevara, A., K. J. Hurme, R. Elting, and A. L. Russell. 2021. Bene“fit” assessment in pollination coevolution: Mechanistic perspectives on hummingbird bill–flower matching. *Integrative and Comparative Biology* 61: 681–695.
- Rolfe, S., S. Pieper, A. Porto, K. Diamond, J. Winchester, S. Shan, H. Kirveslahti, et al. 2021. SlicerMorph: An open and extensible platform to retrieve, visualize and analyse 3D morphology. *Methods in Ecology and Evolution* 12: 1816–1825.
- Royaert, S., W. Phillips-Mora, A. M. A. Leal, K. Cariaga, J. S. Brown, D. N. Kuhn, R. J. Schnell, and J. C. Motamayor. 2011. Identification of marker-trait associations for self-compatibility in a segregating mapping population of *Theobroma cacao* L. *Tree Genetics and Genomes* 7: 1159–1168.
- Salazar-Díaz, R., and V. Torres-Coto. 2017. Estudio de la dinámica de polinizadores del cultivo de cacao (*Theobroma cacao*) en tres sistemas de producción. *Revista Tecnología En Marcha* 30: 90.
- Santos, R. C., J. L. Pires, and R. X. Correa. 2012. Morphological characterization of leaf, flower, fruit and seed traits among Brazilian *Theobroma* L. species. *Genetic Resources and Crop Evolution* 59: 327–345.

- Savriama, Y. 2018. A step-by-step guide for geometric morphometrics of floral symmetry. *Frontiers in Plant Science* 9: 1433.
- Savriama, Y., and D. Tautz. 2022. Testing the accuracy of 3D automatic landmarking via genome-wide association studies. *G3: Genes, Genomes, Genetics* 12: jkab443.
- Simpson, B. B., and J. L. Neff. 1981. Floral rewards: Alternatives to pollen and nectar. *Annals of the Missouri Botanical Garden* 68: 301–322.
- Smith, J. M., R. Burian, S. Kauffman, P. Alberch, J. Campbell, B. Goodwin, R. Lande, et al. 1985. Developmental constraints and evolution: A perspective from the Mountain Lake Conference on development and evolution. *Quarterly Review of Biology* 60: 265–287.
- Staedler, Y. M., T. Kreisberger, S. Manafzadeh, M. Chartier, S. Handschuh, S. Pamperl, S. Sontag, et al. 2018. Novel computed tomography-based tools reliably quantify plant reproductive investment. *Journal of Experimental Botany* 69: 525–535.
- Swanson, J. D. 2005. Flower development in *Theobroma cacao* L.: An assessment of morphological and molecular conservation of floral development between *Arabidopsis thaliana* and *Theobroma cacao*. PhD thesis, Pennsylvania State University, University Park, Pennsylvania, USA.
- Swanson, J. D., J. E. Carlson, and M. J. Guiltinan. 2008. Comparative flower development in *Theobroma cacao* based on temporal morphological indicators. *International Journal of Plant Sciences* 169: 1187–1199.
- Tatsuta, H., K. H. Takahashi, and Y. Sakamaki. 2018. Geometric morphometrics in entomology: Basics and applications. *Entomological Science* 21: 164–184.
- Toledo-Hernández, M., T. C. Wanger, and T. Tschardt. 2017. Neglected pollinators: Can enhanced pollination services improve cocoa yields? A review. *Agriculture, Ecosystems and Environment* 247: 137–148.
- Toledo-Hernández, M., T. Tschardt, T. Aiyen, A. Alam, C. Basir, and T. C. Wanger. 2021. Landscape and farm-level management for conservation of potential pollinators in Indonesian cocoa agroforests. *Biological Conservation* 257: 109106.
- Tripathi, A., D. K. Tripathi, D. K. Chauhan, N. Kumar, and G. S. Singh. 2016. Paradigms of climate change impacts on some major food sources of the world: A review on current knowledge and future prospects. *Agriculture, Ecosystems and Environment* 216: 356–373.
- van der Kooij, C. J., A. G. Dyer, P. G. Kevan, and K. Lunau. 2019. Functional significance of the optical properties of flowers for visual signalling. *Annals of Botany* 123: 263–276.
- van der Niet, T., C. P. E. Zollikofer, M. S. P. de León, S. D. Johnson, and H. P. Linder. 2010. Three-dimensional geometric morphometrics for studying floral shape variation. *Trends in Plant Science* 15: 423–426.
- Vansynghel, J., C. Ocampo-Ariza, B. Maas, E. A. Martin, E. Thomas, T. Hanf-Dressler, N.-C. Schumacher, et al. 2022. Cocoa flower visitation: Low pollen deposition, low fruit set and dominance of herbivores. *Ecological Solutions and Evidence* 3: e12140.
- Verstraete, B., H. K. Moon, E. Smets, and S. Huysmans. 2014. Orbicules in flowering plants: A phylogenetic perspective on their form and function. *Botanical Review* 80: 107–134.
- Vogel, S. 2000. The floral nectaries of Malvaceae sensu lato: A conspectus. *Kutziana* 28: 155–171.
- Wang, C. N., H. C. Hsu, C. C. Wang, T. K. Lee, and Y. F. Kuo. 2015. Quantifying floral shape variation in 3D using microcomputed tomography: A case study of a hybrid line between actinomorphic and zygomorphic flowers. *Frontiers in Plant Science* 6: 724.
- Wanger, T. C., F. Dennig, M. Toledo-Hernández, T. Tschardt, and E. F. Lambin. 2021. Cocoa pollination, biodiversity-friendly production, and the global market. *ArXiv* 2112.02877 [Preprint]. Available at: <https://doi.org/10.48550/arXiv.2112.02877> [published 6 December 2021; accessed 15 September 2023].
- Webb, C. J., and D. G. Lloyd. 1986. The avoidance of interference between the presentation of pollen and stigmas in angiosperms II. Herkogamy. *New Zealand Journal of Botany* 24: 163–178.
- Weber, U. K., S. L. Nuismer, and A. Espíndola. 2020. Patterns of floral morphology in relation to climate and floral visitors. *Annals of Botany* 125: 433–445.
- Westerkamp, C., A. Aparecida Soares, and L. P. do Amaral Neto. 2006. Male and female booths with separate entrances in the tiny flowers of *Guazuma ulmifolia* (Malvaceae-Byttnerioideae). I. Structural integration. *Flora: Morphology, Distribution, Functional Ecology of Plants* 201: 389–395.
- Whitlock, B. A., C. Bayer, and D. A. Baum. 2001. Phylogenetic relationships and floral evolution of the Byttnerioideae (“Sterculiaceae” or Malvaceae s.l.) based on sequences of the chloroplast gene, *ndhF*. *Systematic Botany* 26: 420–437.
- Whitney, H. M., M. Kolle, P. Andrew, L. Chittka, U. Steiner, and B. J. Glover. 2009. Floral iridescence, produced by diffractive optics, acts as a cue for animal pollinators. *Science* 323: 130–133.
- Wickham, H. 2016. *ggplot2: Elegant graphics for data analysis*. Springer, New York, New York, USA.
- Wilson, T. C., B. J. Conn, and M. J. Henwood. 2017. Great expectations: Correlations between pollinator assemblages and floral characters in Lamiaceae. *International Journal of Plant Sciences* 178: 170–187.
- Winder, J. A. 1978. Cocoa flower diptera; Their identity, pollinating activity and breeding sites. *International Journal of Pest Management* 24: 5–18.
- Young, A. M. 1983. Seasonal differences in abundance and distribution of cocoa-pollinating midges in relation to flowering and fruit set between shaded and sunny habitats of the La Lola cocoa farm in Costa Rica. *Journal of Applied Ecology* 20: 801.
- Young, A. M. 1985. Studies of cecidomyiid midges (Diptera: Cecidomyiidae) as cocoa pollinators (*Theobroma cacao* L.) in Central America. *Proceedings of the Entomological Society of Washington* 87: 44–79.
- Young, A. M. 2007. *The chocolate tree: A natural history of cacao*. University Press of Florida, Gainesville, Florida, USA.
- Young, A. M., M. Schaller, and M. Strand. 1984. Floral nectaries and trichomes in relation to pollination in some species of *Theobroma* and *Herrania* (Sterculiaceae). *American Journal of Botany* 71: 466–480.
- Young, A. M., E. H. Erickson, M. A. Strand, and B. J. Erickson. 1987. Pollination biology of *Theobroma* and *Herrania* (Sterculiaceae)—I. Floral biology. *International Journal of Tropical Insect Science* 8: 151–164.
- Zarrillo, S., N. Gaikwad, C. Lanaud, T. Powis, C. Viot, I. Lesur, O. Fouet, et al. 2018. The use and domestication of *Theobroma cacao* during the mid-Holocene in the upper Amazon. *Nature Ecology and Evolution* 2: 1879–1888.
- Zhang, D., S. Mischke, E. S., Johnson, W. Phillips-Mora, and L. Meinhardt. 2009. Molecular characterization of an international cacao collection using microsatellite markers. *Tree Genetics and Genomes* 5: 1–10.

SUPPORTING INFORMATION

Additional supporting information can be found online in the Supporting Information section at the end of this article.

Appendix S1. Specimen collection information.

Appendix S2. CT scan records for flowers and hypothesized pollinators.

Appendix S3. Photographic guide to the specimen positioning techniques used.

Appendix S4. Raw landmark data set for all specimens.

Appendix S5. Floral shape outliers plot.

Appendix S6. Procrustes ANOVA results.

How to cite this article: Wolcott, K. A., E. L. Stanley, O. A. Gutierrez, S. Wuchty, and B. A. Whitlock. 2023. 3D pollination biology using micro-computed tomography and geometric morphometrics in *Theobroma cacao*. *Applications in Plant Sciences* 11(5): e11549. <https://doi.org/10.1002/aps3.11549>